INNSPUB

Journal of Biodiversity and Environmental Sciences (JBES)
ISSN: 2220-6663 (Print) 2222-3045 (Online)
Vol. 14, No. 5, p. 1-12, 2019
http://www.innspub.net

RESEARCH PAPER OPEN ACCESS

Exergetic analysis and optimization of a flat plate solar collector

Bouragbi Lakhdar[1], Azzouz Salaheddine[1], Mahfoud Brahim[2], Djidel Mohamed[*3]

[1]*Mechanical Laboratory of Materials and Industrial Maintenance (LR3MI), Badji Mokhtar University, Annaba, Algeria*

[2]*Département de Génie Mécanique, Université de Bouira, Bouira, Algeria*

[3]*Laboratoire de Géologie du Sahara, Université Kasdi Merbah Ouargla, Ouargla, Algérie*

Article published on May 30, 2019

Key words: Flat-plate solar collector, Exergy, Entropy generation, Optimal efficiency, Irreversibility.

Abstract

Energy efficiency based on the first law of thermodynamics is generally used as one of the most important parameters for evaluating and comparing thermal systems. Also, losses due to irreversibility or entropy generation of the system, which are derived from the second law of thermodynamics, are usually neglected. Here, the concept of exergy is employed to combine both the laws in the framework of the study of a Flat Plat Solar Collector (FPSC). Indeed, FPSCs suffer from low energy efficiency which is related to many impact factors like heat loss from the absorber to the environment and low conversion of the incident solar energy into thermal energy absorbed by the heat transfer fluid. In this study, an exergetic analysis of a FPSC used in Saharan conditions is carried out in order to minimize the destroyed exergy (irreversibility) and to obtain the optimal operating parameters of the FPSC that maximize both the exergy and the energy efficiencies. The results reveal that the optimal exergy efficiency is of 8.28% and the optimal mass flow rate is of 0.06 kg/s. This finding and the assumptions made for the calculation approach are discussed with regard to other performed studies.

***Corresponding Author:** Djidel Mohamed ✉ djidelm@yahoo.fr

Introduction

The global crisis of fossil fuels especially of oil is still persistent and strongly depends on its increasing exploitation. Three main challenging situations that affect the strategies of the countries relative to energy consumption and to the operation of renewable energies are distinguished. Environmental problems, unstable fossil fuel markets and depletion of fossil fuel resources push governments to follow a new strategy as alternative solution to energy consumption by renewable energies (Eugene *et al*, 2014). The solar energy presents the most useful form of renewable energy as it is freely available and can provide tremendous potential to satisfy a large part of the world's energy demand. This energy can be either converted into electricity or heat (Soteris, 2004).

A domestic solar water heating system is one of the most widely recognized solar applications, where solar radiation energy is converted into thermal energy to heat water. In these systems, the most important element is the solar collector, such as the Flat Plate Solar Collector (FPSC) that plays an essential role in the recovery and the conversion of solar radiations. Thus, optimization of its different operating parameters is an interesting challenge. In some domains of application, FPSCs are advantageous compared to parabolic and cylindroparabolic solar collectors, due to the low operating temperature range of up to 150°C and their simple design. These domains include solar heating devices, solar water desalination systems, solar air conditioners and refrigerators and solar drying processes (Saidur *et al*, 2012).

Performances of FPSCs are affected by various climatic factors as well as by the design and the operating parameters (Soteris, 2004): solar radiation, orientation and inclination of the collector, ambient temperature, relative humidity, wind speed, selective coating and absorber construction material, tube and fin profile, number and type of glazing, insulation material, thermophysical properties of the heat transfer medium, inlet and outlet temperature, mass flow rate and overall loss coefficient. The desert climate presents specific factors that influence on the photothermal conversion of solar collectors (plane, parabolic, parabolic trough) and equally on the photovoltaic conversion of photovoltaic solar panels. Among these factors, one can quote the dust deposition due to storms, the degradation of solar collector surfaces (transparent roofs, photovoltaic panels and reflector mirrors) owing to sandstorms which increase roughness and modify optical properties. These two causes have been widely studied to appreciate their impacts on the thermal and photovoltaic performances of solar collectors (Said, 1990; Semaouia *et al*., 2015). In the last decade, the combination of energy and exergy analyses has been envisaged in several studies to understand and optimize FPSCs. The Hottel-Whillier-Bliss model that combines most of the factors affecting a FPSC is presented by Struckmann (2008). The role of thermal efficiency to describe the energetic performance of this collector is shown. However, this study is only based on the energetic analysis, i.e. the First Law of Thermodynamic (FLT) and needs to be completed by a deep study by taking into account the energetic losses regarding the internal and external irreversibility (entropy generation) within the system and with its environment.

Dincer and Rosen (2013) announced that after the FLT, the quantities of energy converted from one form to another in any process, are conserved independently of the feasibility of the process. The second law of thermodynamics deals with the quality of energy which can occasion change, degradation of energy during a process, entropy generation and lost opportunities to produce work (Hepbasli, 2008). In addition, authors reported the concept of exergy analysis so as to analyze, design and improve the energy transfer by joining both the laws of thermodynamics (Dincer and Rosen, 2013). This concept will be further used in the present paper. Moreover, the latter concept has been utilized by research workers to compare energy behaviors in the context of exergy studies of FPSCs referring to offered opportunities. The pros and cons of different configurations have been highlighted such as for the

passage section of the fluid in the absorber tubes (Benli, 2013), the shape and the assembling of the fins with the absorber tubes (Wencelas and Tchuen, 2017), the design of the FPSC (Tohching *et al*, 2007) and the variations of the heat transfer fluids (Shojaeizadeh and Veysi, 2016; Verma *et al*., 2017; Alim *et al*., 2016).

Additionally, Kalogirou *et al.* (2016) present a study of the exergy analysis of a solar thermal collector and of other solar thermal systems. This analysis gives an attractive and representative method to evaluate the performance of these systems with different configurations. This approach can then be employed when the solar collector is considered alone or with its environment to identify the sources of irreversibilities. Besides, Luminosu and Fara (2005) showcase a numerical simulation to discuss the optimal performance of a FPSC by using the exergy analysis. Although valuable results are acquired, their study only deals with the case where the inlet temperature of the fluid (T_{fi}) is assumed constant and equal to the ambient temperature ($T_{fi} = T_a = const$). Also, based on the equation of exergy efficiency, the exergy flux is considered equal to the one of the solar radiation and the destroyed exergy is not accounted for. Subsequently, the irreversible losses are neglected.

Even though Farahat *et al.* (2009) used the same procedures, their case study was based on the equality of T_{fi} and T_a. So, satisfactory results were found as they took into consideration the points disregarded by Luminosu and Fara (2005). On another note, Singh *et al.* (2016) conducted a thermal and exergy study of a solar water heater manufactured and tested under the Allahabad (India) climatic conditions for a fixed mass flow rate of 0.0015 kg/s. They obtained a fluid outlet temperature of 55°C and a daily efficiency of 11%. Nevertheless, the study lacks an exergetic optimization to find and examine the optimal values of this prototype.

Lastly, Das (2016) propounded a numerical simulation of six solar collectors using a program developed in "C" language to evaluate and compare their optimal operating parameters. He held significant results: an optimal mass flow rate varied from 0.0019 to 0.0022 kg/s and an optimal exergy efficiency varied from 5.2% to 8.2%. However, he dealt with a particular case for which the inlet temperature of the fluid is assumed equal to the ambient temperature, that is $T_{fi} \cong T_a$.

As a follow-up to these investigations, the thermal behavior of a flat plate solar collector (FPSC) under Saharan climatic conditions is investigated. An exergy analysis is undertaken to determine the optimum values of the mass flow rate, the maximum exergy efficiency and the minimum of the exergy destroyed (entropy generation). To achieve these three objectives, the next research plan is adopted. The operating principle of the considered system and the assumptions made with respect to the quoted approaches are exhibited to begin with. The thermodynamic equations of the energy and exergy balance are then detailed with a focus on the approach to retrieve the exergetic efficiency. The optimization is searched by minimizing the destroyed exergy from the expression of the exergetic efficiency. The calculation method to solve the equations of the model is displayed and then applied to the characteristics and measurements realized with a solar collector used under desert climatic condition. To round off, the found results are discussed and conclusions are drawn.

Material and methods

Studied system and assumptions

The case of a FPSC to heat water with greenhouse and thermosiphon phenomena is treated. This kind of exchanger converts solar radiation energy into internal heat energy by means of the transport medium, a fluid which is usually water. The main components of the FPSC are (Fig. 1): (1) a metal frame, (2) an insulation to minimize heat losses, (3) a flat plate absorber with fluid circulation passageways and (4) a transparent cover to allow transmission of solar energy into the enclosure. More details can be found in (Sukhatme and Nayak, 2017). The ensuing key points are taken into account in the study being conducted.

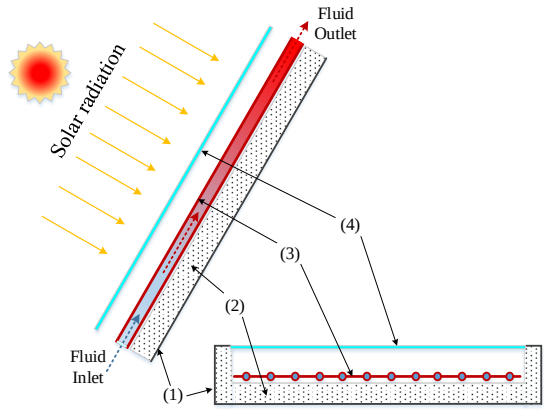

(1) Casing. (2) Insultions. (3) Absorber. (4) Glazing

Fig. 1. Principle of the flat plate solar collector.

The inlet temperature of the fluid is different from the ambient temperature, $T_{fi} \neq T_a$, which is a real advantageous case during the design phase of the FPSC. In practice, it represents a broader situation than the limited case where $T_{fi} \cong T_a$ as assumed by Luminosu and Fara (2005), Farahat *et al.* (2009), Singh *et al.* (2016) and Das (2016). Indeed, the exergetic analysis, that takes into consideration the system and its environment is not well suited to this hypothesis. More specifically, the environmental temperature T_a is an important parameter in the exergetic relations. Any error in the ambient temperature value ($T_a \pm \Delta T$) directly affects the calculation of the optimum values of the FPSC. The studied FPSC is a solar water heater with a thermosiphon that works in Saharan climatic conditions. The solar irradiance reached 1100 W/m² and the temperature 35°C on our test day. By constituting an accessible analytical method for the exergy analysis, we attempt to determine the optimal exergetic efficiency.

Equations for analysis

Energy

Under steady-state conditions and based on the first law of thermodynamics, the energy balance of the FPSC is formulated as:

$Q_s = Q_u + Q_l$ (1)

Where Q_s is the rate of solar energy absorbed by the plate per unit area, Q_u is the rate of useful energy transferred to the fluid and Q_l is the rate of the energy lost per unit area by the absorber plate to the surroundings.

The expression of the energy of the solar radiation absorbed by the absorber Q_s, which depends on the location, the orientation and the inclination of the collector is given by:

$$Q_s = G^*(\tau\alpha)A \qquad (2)$$

The heat losses Q_l, from the absorber to the environment, can be expressed in a linear form by the model of Hottel-Whillier-Bliss which is the commonly used model for a FPSC (Feidt, 1987):

$$Q_l = UA(T_w - T_a) \quad (3)$$

The rate of the useful thermal energy Q_u represents the enthalpy variation of the fluid from the inlet to the outlet. This fluid has a specific heat at constant pressure C_p, a mass flow rate $\dot{m}$ and its temperature varies from T_{fi} to T_{fo} in the FPSC:

$$Q_u = \dot{m}C_p(T_{fo} - T_{fi}) \qquad (4)$$

Therefore, the energy balance equation (1) can be written as:

$$\dot{m}C_p(T_{fo} - T_{fi}) = A(\tau\alpha)G^* - UA(T_w - T_a) \qquad (5)$$

The overall thermal efficiency of the FPSC, obtained by dividing the amount of useful energy Q_u by the energy of solar radiation absorbed Q_s, is:

$$\eta_{en} = \frac{Q_u}{Q_s} = \frac{\dot{m}C_p(T_{fo} - T_{fi})}{(\tau\alpha)AG^*} \qquad (6)$$

Exergy

The exergy of a system, as defined in (Dincer and Rosen, 2013), represents the maximum work that can be realized by the system and its environment (Fig. 2). This reference environment is assumed to be infinite, in equilibrium. It contains all the other systems and is totally specified by stating its temperature, pressure and chemical composition (Dincer and Rosen, 2013). For the process evolving between two temperatures (source T and environment T_a), the maximum work W_{max} produced during this process, is given by:

$$W_{max} = Ex = \left(1 - \frac{T_a}{T}\right)Q = \beta Q \qquad (7)$$

One can see that Q is the thermal energy available at the temperature T and $(\beta = 1 - T_a/T)$ where β represents Carnot's thermal efficiency between the source temperature T and the sink one T_a which is responsible for high-grade energy (Tiwari and Shyam, 2016).

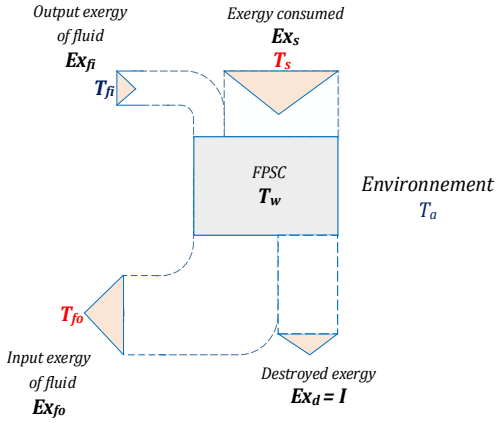

Fig. 2. Exergy flow diagram of the FPSC.

In general, for a thermo-mechanical system, whose energy consists of internal energy, macroscopic kinetic energy and gravitational potential energy, the expression of exergy can be easily written as (Lallemand, 2007):

$$Ex = E_{in} + E_k + E_{po} - T_a S - P_a V - \sum_i \mu_{ia} N_i \quad (8)$$

Thus, the exergy balance of the FPSC, which includes the exergy input, the exergy output and the exergy destroyed from the system (FPSC) is given below:

$$\sum Ex_i - \sum Ex_o = \sum Ex_d \quad (9)$$

$$Ex_s + \dot{m} \cdot ex_{fi} - \dot{m} \cdot ex_{fo} = Ex_d \quad (10)$$

The exergy input consists of two parts: the exergy input carried by the heat transfer fluid and the exergy of solar radiation absorbed by the FPSC.

In the first part, the exergy inlet of the fluid at the input of the collector is (Bejan, 1988):

$$Ex_{fi} = \dot{m} \cdot ex_{fi} = \dot{m} C_p \left[T_{fi} - T_a - T_a \ln\left(\frac{T_{fi}}{T_a}\right)\right] \quad (11)$$

The second part, which is called the exergy consumed by the system, is the solar exergy that can be derived from the amount of energy Q_s between the temperatures T_a and T_s. It is calculated by using one of the following equations presented by Spanner (1964), Petela (1964) and Jeter (1981) respectively:

$$Ex_s = Q_s \left[1 - \frac{4T_a}{3T_s}\right] \quad (12)$$

$$Ex_s = Q_s \left[1 + \frac{1}{3}\left(\frac{T_a}{T_s}\right)^4 - \frac{4T_a}{3T_s}\right] \quad (13)$$

$$Ex_s = Q_s \left[1 - \frac{T_a}{T_s}\right] \quad (14)$$

Where T_s is the temperature of a blackbody, which has a spectrum alike the sun. Note that several authors have approximately used the value T_s equal to 5780°C as mentioned in (Feidt, 1987). For an ambient temperature (maximum assumed) below or equal to 60°C, differences in the calculation values resulting from these three correlations should not exceed 1.5%. Jeter's expression (14) is employed in our calculation because of its simplicity and its similarity to relationship (7).

The output exergy is only constituted of the fluid exergy at the output of the collector, which is given by (Bejan, 1988):

$$Ex_{fo} = \dot{m} \cdot ex_{fo} = \dot{m} C_p \left[T_{fo} - T_a - T_a \ln\left(\frac{T_{fo}}{T_a}\right)\right] \quad (15)$$

However, the useful exergy is obtained by subtracting (10) from (14) as follows:

$$Ex_u = Ex_{fo} - Ex_{fi} = \dot{m}(ex_{fo} - ex_{fo}) = \dot{m} C_p \left[(T_{fo} - T_{fi}) - T_a \ln\left(\frac{T_{fo}}{T_{fi}}\right)\right] \quad (16)$$

The last member of exergy balance Ex_d represents the exergy destroyed or the irreversibility rate I of the system, which is called the Gouy–Stodola relation (Dincer and Rosen, 2013):

$$Ex_d = I = T_a S_{ge} \quad (17)$$

Overall, due to the difference in temperature and without taking the frictional pressure drop of the fluid, the lost (destroyed) exergy Ex_d is generated in three processes according to Suzuki (1988):

– absorption exergy loss (radiation → plate): an exergy annihilation process when the solar radiation at T_s is absorbed by the absorber at T_w.
– leakage exergy loss (plate → ambient): an exergy loss process accompanied with heat leakage from the absorber T_w out into its surroundings T_a.

– conduction exergy loss (plate → fluid): an exergy annihilation process caused by heat conduction between the absorber T_w and the heat transfer fluid T_f.

By substituting expressions (14), (16) and (17) in the relation of the exergy balance (10), we get:

$$I = T_a S_{cr} = Q_s\left(1 - \frac{T_a}{T_s}\right) + \dot{m}C_p\left(\left(T_{fo} - T_{fi}\right) - T_a \ln\left(\frac{T_{fo}}{T_{fi}}\right)\right) \quad (18)$$

Therefore,

$$Ex_d = Ex_s - Ex_u \quad (19)$$

By definition, the exergy efficiency is the ratio of exergy output to exergy input:

$$\eta_{ex} = \frac{Ex_o}{Ex_i} \quad (20)$$

By using the exergy balance relation (9), we have:

$$\eta_{ex} = \frac{Ex_o}{Ex_i} = 1 - \frac{Ex_d}{Ex_i} \quad (21)$$

In addition, by using the exergy balance supplied by relation (19), the exergy efficiency of a system can be represented by the ratio between the useful exergy produced Ex_u and the exergy consumed by the system Ex_{sol}.

$$\eta_{ex} = \frac{Ex_u}{Ex_s} \quad (22)$$

Or, equivalently:

$$\eta_{ex} = \frac{\dot{m}C_p\left(\left(T_{fo} - T_{fi}\right) - T_a \ln\left(\frac{T_{fo}}{T_{fi}}\right)\right)}{(\tau\alpha)AG^*\left(1 - \frac{T_a}{T_s}\right)} \quad (23)$$

Dimensionless expressions

Aiming at simplifying the preceding equations as well as the exergy analysis of the system, the expressions are rewritten in a dimensionless form using the following dimensionless relations:

$$\theta_w = \frac{T_p}{T_a} - 1, \theta_{fi} = \frac{T_{fi}}{T_a} - 1, \theta_{fo} = \frac{T_{fo}}{T_a} - 1, \theta_s = \frac{T_s}{T_a} - 1 \text{ and } \theta_{max} = \frac{T_{max}}{T_a} - 1 \quad (24)$$

Which represent respectively the absorbing wall temperature, the inlet fluid temperature, the outlet fluid temperature, the apparent sun temperature and the maximum collector temperature.

After replacement and simplification, the equation of the energy balance (5) becomes:

$$M\left(\theta_{fo} - \theta_{fi}\right) = 1 - \frac{\theta_w}{\theta_{max}} \quad (25)$$

Where

$M = \frac{\dot{m}C_p}{Q_s/T_a}$ is the dimensionless mass flow number.

$\theta_{max} = \frac{(Q_s/T_a)}{UA}$ is the dimensionless maximum collector temperature, which is achieved at the stagnation temperature of $T_{fo}=T_{fi}$.

The energy efficiency is in this case given by:

$$\eta_{en} = M\left(\theta_{fo} - \theta_{fi}\right) \quad (26)$$

After substitution and simplification, we are left with:

$$N_s = \frac{\theta_s}{\theta_s + 1} - M\left(\theta_{fo} - \theta_{fi}\right) + M \ln\frac{\theta_{fo}+1}{\theta_{fi}+1} \quad (27)$$

That is:

$$N_s = N_{Exs} - N_{Exu} \quad (28)$$

Where

- $N_S = \frac{T_a S_{cr}}{Q_s}$ is the number of entropy generation or the dimensionless exergy destroyed.
- $N_{Exs} = \frac{\theta_s}{\theta_s + 1}$ is the dimensionless exergy emitted from the sun to the collector.
- $N_{Exu} = M\left(\theta_{fo} - \theta_{fi}\right) - M \ln\frac{\theta_{fo}+1}{\theta_{fi}+1}$ is the useful dimensionless exergy.

Finally, the exergy efficiency of the collector in the following dimensionless form is:

$$\eta_{ex} = \frac{N_{Exu}}{N_{Exs}} = 1 - \frac{N_s}{N_{Exs}} \quad (29)$$

or likewise:

$$\eta_{ex} = \frac{M\left(\theta_{fo} - \theta_{fi}\right) - M \ln\frac{\theta_{fo}+1}{\theta_{fi}+1}}{\frac{\theta_s}{\theta_s + 1}} \quad (30)$$

Optimization approach

The useful exergy can be improved by increasing the mass flow rate of the fluid through the collector. However, for high mass flow rates, the outlet temperature of the fluid becomes very low. On the other hand, for reduced flow rates, the outlet temperature becomes very high, which results in the

raise of the exergy losses (destroyed exergy). These remarks make the optimization of the mass flow a necessary point to improve the performance of the FPSC system.

Bejan *et al.* (1981) announced that: "The task of maximizing the energy, delivered by a collector of fixed cross-section Ac, is equivalent to minimizing the rate of entropy generation in the "column" of cross-section Ac extending from the environment temperature (T_a) to the apparent sun temperature as an energy source (T_s)". Therefore, the performance of the FPSC can be optimized by finding the exergy efficiency and the mass flow rate of the fluid corresponding to the minimization of the entropy generation number, i.e., the following maximum exergy extraction:

$$\frac{d\eta_{ex}}{dM} = \frac{dN_{Exu}}{dM} = \frac{dN_S}{dM} = 0 \quad (31)$$

Solving the minimization equation ($(dN_S)/dM=0$) yields to the optimum collector mass flow rate for the minimum irreversibility. However, the entropy generation number N_S is a function of the mass flow rate M and of the outlet temperature θ_{fo} of the FPSC, in other words $N_S=f(M,\theta_{fo})$. Furthermore, these two variables (M,θ_{fo}) are interdependent and in relation to the temperature profile of the absorber along the direction of the fluid flow. In view of (Tiwari and Shyam, 2016), we get:

$$\frac{T_{fo}-T_a-\frac{Q_S}{UA}}{T_{fi}-T_a-\frac{Q_S}{UA}} = exp\left(-\frac{UA\acute{F}}{\dot{m}C_p}\right) \quad (32)$$

In its dimensionless form, it can also be written as:

$$\frac{\theta_{fo}-\theta_{max}}{\theta_{fi}-\theta_{max}} = exp\left(-\frac{\acute{F}}{M\theta_{max}}\right) \quad (33)$$

According to relation (31), the maximum of useful exergy is equivalent to the minimum of the destroyed exergy or to the minimum of irreversibility of the system:

$$\frac{dN_{Exu}}{dM} = \frac{d}{dM}\left[M\left(\theta_{fo}-\theta_{fi}-\ln\frac{\theta_{fo}+1}{\theta_{fi}+1}\right)\right] = 0 \quad (34)$$

Similarly, we have:

$$\theta_{fo}-\theta_{fi}-ln\frac{\theta_{fo}+1}{\theta_{fi}+1}+M\frac{\theta_{fo}}{\theta_{fi}+1}\frac{d\theta_{fo}}{dM} = 0 \quad (35)$$

By replacing in equation (34) the result of the derivative of θ_{fo} with respect to M which is procured from equation (32) of the temperature profile of the absorber, the expression below is deduced:

$$\theta_{fo}-\theta_{fi}-ln\frac{\theta_{fo}+1}{\theta_{fi}+1}-\frac{\theta_{fo}(\theta_{fo}-\theta_{max})}{\theta_{fo}+1}ln\frac{\theta_{fo}-\theta_{max}}{\theta_{fi}-\theta_{max}} = 0 \quad (36)$$

Finally, the expression achieved is a non-linear equation that links the maximum (stagnation) temperature θ_{max} with the inlet and the outlet temperatures $(\theta_{fi},\theta_{fo})$ of the fluid. Since both the parameters θ_{fi} and θ_{fo} are known from the measurements taken on the FPSC, equation (36) can be written as underneath:

$$(\theta_{fo}-\theta_{max})\ln\frac{\theta_{fo}-\theta_{max}}{\theta_{fi}-\theta_{max}}+C = 0 \quad (37)$$

Where:

$$C = \frac{\theta_{fo}-\theta_{fi}-\ln\frac{\theta_{fo}+1}{\theta_{fi}+1}}{\frac{-\theta_{fo}}{\theta_{fo}+1}} = f(\theta_{fi},\theta_{fo}) \quad (38)$$

FPSC characteristics and calculations

The solar collector used here is a thermosiphon solar water heater that was subjected to a series of tests and measurements to determine its performance on the testing platform at the Renewable Energy Research Center (CDER) of the Adrar unit in Saharan environment. Table 1 shows the technical characteristics of this solar collector. The description of the test report, of the location environment and of the measurement results are presented in the study performed by Bennaceur *et al.* (2010).

Table 1. Technical data of the solar collector.

Component	Dimensions and specifications	Material
Casing	Length: 1.930 m Width: 0.9 m Height: 0.08 m	Aluminum
Glass cover	Thickness: 0.004 m Transmissivity: 0.88 Refractive index: 1.52	White glass
Absorber	Absorber type Thickness: 0,6.10-3m Emissivity: 0.2 Thermal conductivity 240 W/m.°C Absorptivity: 0.95 Diameter: 0.012/0.014m Number of tubes: 9	Fin-Tube Aluminum Copper
Collector	Length: 1 m Diameter: 0.020/0.022 m Number : 2	Copper
Insulation	Back thickness: 0.03 m Lateral thickness: 0.03 m Thermal conductivity: 0.0027 W/m.°C	

The measurements were carried out in Adrar located in the mid Saharan part of Algeria. The site coordinates are: latitude 27.88°, longitude 0.28° and altitude 264m with an albedo 0.2. The FPSC is inclined at 27° with a South face orientation. The measurements were taken during a test day, on 7 April 2005 with the following instruments: type K (Chromel-Alumel) thermocouples to measure the temperatures with high resolution ±0.02°C and a Kipp and Zonen type pyranometer to measure the global solar irradiance with a resolution of ±1%. For data logging, a Fluke 2625A recorder was programmed to register the temperatures and the global solar irradiance with a one-minute time step.

From the measured values of the temperatures and the global solar irradiance, the dimensionless temperatures are calculated as a function of the relationships (24). Expression (36) gives for each series of measurements a nonlinear equation with a variable θ_{max}. For solving these equations, a program is developed with MATLAB software employing the 'solve' function. Then, all the other parameters such as $(M_{op}, \dot{m}_{op}, N_{Exs}, N_{Exu(op)}, N_{s(op)}, \eta_{ex(op)}$ and $, \eta_{en(op)})$ are calculated by using expressions (25) to (30).

Result and discussion

The measurement and calculation results are grouped in Tables 2 and 3. Please refer to the text for the notation used in those tables. In the last two lines of Table 3, the negative values are due to the very close inlet and outlet fluid temperatures ($T_{fi} \cong T_{fo}$=35°C) and to the low solar irradiance (22 W/(m²)). On the other hand, in the last row, the undetermined values are owing to the equal temperatures ($T_a \cong T_{fi}=T_{fo}$=27°C) and to the absence of solar irradiance for this hour. These two points can be explained by the thermal equilibrium between the solar collector and its environment.

Table 2. Data measurement.

Hour [h]	G^* [W/m^2]	T_a [°C]	T_{fi} [°C]	T_{fo} [°C]	T_{wm} [°C]
10:00	815	24.5	36	56	40.5
11:00	1000	26.5	44	67.5	49.00
12:00	1100	28.5	51	74.5	55.5
13:00	1095	29.5	57	80	61.00
14:00	1025	32	64	84	65.25
15:00	880	34	68	84	66.75
16:00	680	34.5	72	83	67.50
17:00	418	35	73	76.5	64.25
18:00	85.5	32	54	55	54.75
19:00	22	31	35	35.3	50.00
20:00	0	26	27	27	40.75

Table 3. Calculated parameters.

Hour [h]	θ_s [−]	θ_{fi} [−]	θ_{fo} [−]	θ_{wm} [−]	θ_{max} [−]	M_{op} [−]	$\dot{m}_{op}$ [kg/s]	N_{Exs} [−]	$N_{Exu(opt)}$ [−]	$N_{s(op)}$ [−]	$\eta_{ex(op)}$ [%]	$\eta_{en(op)}$ [%]
10:00	19.34	0.0387	0.1059	0,0538	0.176	10.327	0.0207	0.950	0.046	0.904	4.90	69.43
11:00	19.21	0.0584	0.1369	0,0751	0.235	8.676	0.0212	0.950	0.060	0.890	6.34	68.08
12:00	19.07	0.0746	0.1526	0,0896	0.270	8.580	0.0229	0.951	0.068	0.882	7.15	66.88
13:00	19.01	0.0909	0.1669	0,1041	0.304	8.656	0.0229	0.950	0.075	0.875	7.89	65.81
14:00	18.84	0.1049	0.1705	0,1090	0.320	10.052	0.0247	0.949	0.079	0.870	8.38	65.92
15:00	18.71	0.1107	0.1629	0,1067	0.312	12.621	0.0264	0.949	0.079	0.870	8.33	65.78
16:00	18.68	0.1220	0.1577	0,1073	0.316	18.463	0.0298	0.949	0.081	0.868	8.53	66.05
17:00	18.65	0.1234	0.1347	0,0950	0.304	60.493	0.0600	0.949	0.078	0.870	8.28	68.74
18:00	18.84	0.0721	0.0754	0,0746	0.135	136.83	0.0280	0.949	0.031	0.919	3.25	44.86
19:00	18.91	0.0132	0.0141	0,0625	0.006	-9850	-0.521	0.949	-0.13	1.081	-13.8	-972
20:00	19.24	0.0033	0.0033	0,0493	0	-	-	0.950	-	-	-	-

Fig. 3 shows the measured exergy during the test day. Each group of bars in this Figure. represents the exergy balance as a function of time. The highest bars denote the solar exergy Ex_s consumed by the FPSC. The amount of this solar exergy, which is transferred to the fluid, corresponds to the useful exergy Ex_u, and the remaining part to the exergy destroyed by the collector Ex_d. According to how the tops of these bars change, the useful exergy is always inferior to the solar exergy and superior to destroyed one until the exergetic balance, for which the difference of exergy becomes null Ex_s-Ex_d=0. Indeed, when Ex_s=Ex_d, all the consumed exergy is destroyed by the collector or Ex_s=Ex_d=0; both the quantities are equal to zero when there is no solar irradiance.

Fig. 4 depicts the variation of the inlet θ_{fi} and outlet θ_{fo} dimensionless temperatures of the fluid and the stagnation temperature θ_{max} of the solar collector during the test day, from 10am to 8pm.

The dimensionless temperature can be split into two domains: from 10am to 5pm and from 5 pm to sunset time.

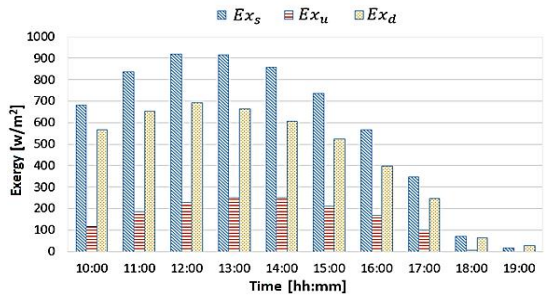

Fig. 3. Exergy measured during the test day.

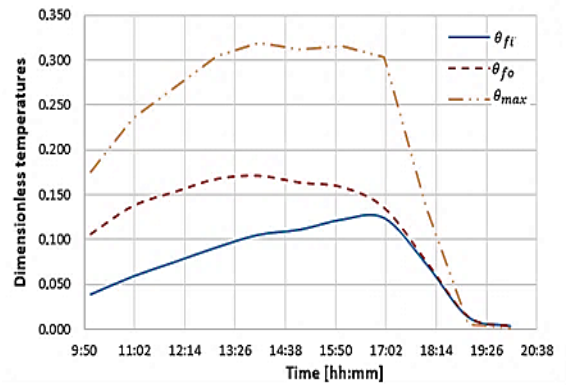

Fig. 4. Dimensionless temperature of the solar collector during the test day.

The first zone is defined from 10 am to 5pm. On one hand, there is a difference of temperature between the inlet and the outlet of the collector, which varies from 20°C to 25°C (+5°C) between 10 am to 1 pm and from 25°C to 4°C (-21°C) between 1pm to 5pm. On the other hand, the stagnation temperature θ_{max} augments from 10am to 1pm by 44°C and goes on with a nearly constant difference of 7°C from 1 pm to 5pm. These temperature differences are very important as they show the energy gain that the fluid can absorb in a desert region (Saharan environment, Adrar in Algeria) with high solar irradiance during spring.

The second domain commences at 5pm. The two curves of θ_{fi} and θ_{fo} converge and coincide following the thermal balance owing to the diminution of the heat absorption of the absorber because of limited solar irradiance. The two curves match after 6 pm. For the stagnation temperature, there is a faster decrease towards the point of exergy equilibrium, for which the amount of consumed exergy is completely destroyed by the FPSC. At this point, the flow direction of the fluid, generated by the thermosiphon, can be reversed because the useful exergy is zero. The absorber becomes a cold source and the reservoir a hot one.

Fig. 5 displays the increase of the mass flow with a low rate up to 4 pm. The temperatures T_a, T_{fi} and T_{fo} stand for respectively the ambient temperature, the inlet and the outlet ones. However, the temperature differences T_{fi}-T_a and T_{fo}-T_a are remarkably raised because the solar irradiance is significant during this phase, as its value attains 1025 W/m² at 2pm.

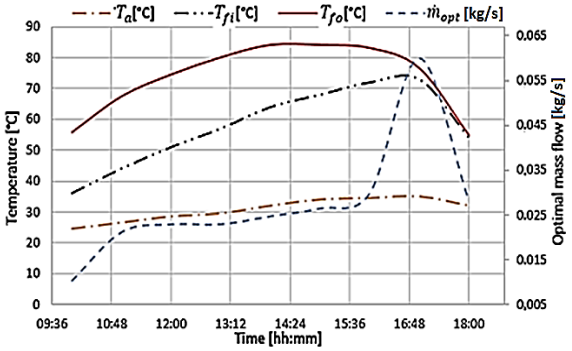

Fig. 5. Variation of temperatures and the optimal mass flow $\dot{m}_{op}$ during the test day.

From 4pm onwards, despite the decrease of the solar irradiance, there is a relevant gain of the mass flow rate in comparison with the previous phase. This is due to the thermal inertia of the FPSC and to the decrease of the destroyed exergy as can evenly be seen in Fig. 3. The mass flow rate continues growing until being at an optimal value of 0.06 kg/s. The latter value accounts for the best performance of the operating point of the collector as it corresponds to the minimum irreversibility of the system. Fig. 6 depicts the variations of the dimensionless inlet and outlet fluid temperatures, the mass flow rate and the number of destroyed exergy. The increase of the mass flow rate leads to an augmentation of the flow velocity of the fluid inside the absorber.

At the beginning, this velocity promotes the heat transfer from the absorber to the fluid, but after the optimum value of the mass flow 0.06kg/s, the heat

transfer is degraded because the solar irradiance gets low between 4pm to 6pm, and the curves of the inlet and outlet temperatures of the fluid (which are still high from 83 to 76°C) are confused. This is due to the thermal balance, which favors the energy losses and the raise of destroyed exergy.

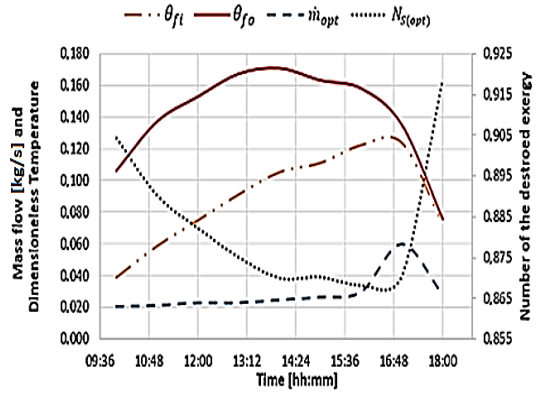

Fig. 6. Variation of the exit temperatures, mass flow and exergy destroyed during the test day.

Table 4 gives the comparison between the exergy and the energy analysis. It can be noticed that the lost energy represents 31.26% of the amount of the solar energy absorbed by the collector whereas the destroyed exergy corresponds to 91.72% of the consumed solar exergy.

The difference between both the percentages which is 60.46% equates to the irreversibility losses in the system, which is not accounted for in the energy balance given that the latter is only based on the FLT which does not consider the entropy generation in the system (solar collector and its environment).

For this purpose, the energy efficiency 68.74% is greater than the exergy efficiency 8.28%. The optimal values obtained are an exergetic efficiency $\eta_{ex(op)}$ =8.28%, an energy efficiency $\eta_{en(op)}$ =68.74% and a mass flow $\dot{m}_{op} = 0.06\ kg/s$.

The latter values are very acceptable compared with other studies such as the one of Ge *et al.* (2014) who found results very close to ours with an exergetic efficiency of 5.96% and a mass flow rate $\dot{m}_{op} = 0.05\ kg/s$ (with T_a=20°C, G*=800 W/m² and T_{fi}=50°CTi).

Table 4. Exergy and energy balance.

Exergy balance		Energy balance	
$N_{s(op)}$	0.9491	Q_s [W/m²]	418
$N_{Exu(op)}$	0.0786	$Q_{util(op)}$[W/m²]	287.375
$N_{S(op)}$	0.8705	$Q_{l(op)}$[W/m²]	130.625
$\eta_{ex(op)}$	8.28 %	$\eta_{en(op)}$	68.74%

The acquired results, such as $\dot{m}_{op} = 0.06\,kg/m^3$, $\eta_{ex(op)} = 8.28\%$, are also very reasonable compared to the obtained ones in (Luminosu and Fara 2005), (Farahat *et al*, 2009) and (Das, 2016) respectively $(\dot{m}_{op} = 0.0021 - 0.0061\,kg/m^3, \eta_{ex(op)} = 3.6\%)$, $(\dot{m}_{op} = 0.0087\,kg/m^3, \eta_{ex(op)} = 3.89\%)$ and $(\dot{m}_{op} = 0.0019 - 0.0022\,kg/m^3$, $\eta_{ex(op)}$ =5.2-8.2%) where they assumed in their studies that $T_{fi} \cong T_a$. This is attributable to the fact that we relied directly on the values recorded during the experiment. The recorded temperatures T_a and T_{fi} are uneven and not close to each other ($T_{fi} > T_a$). Besides, the differences regarding other models, the dimensions of the FPSC and the nature of the desert climate explain the discrepancies between the results. Indeed, the dimensions and the environmental conditions especially the ambient temperature T_a in the exergetic method were the main factors accounted for in our calculations.

It is worth noting that the optimization of the exergetic efficiency of the solar collector gives a great difference of interpretation compared to the energy efficiency. The latter only focuses on the losses with respect to the ambient environment on one side, and on the other one the exergetic efficiency describes all the stages of the energy degradation undergone by the system. The exergy properly quantifies losses and all internal irreversibilities. It allowed us to highlight the strong and the weak energy points of the system and also to carry out the comparison and the choice - especially during the design phase - between the FPSC models that operate under like conditions. Hence, the exercised method could be helpful to the designer to take the right decision.

Conclusion

In this work, a new complete method based on the concept of exergy is presented with a useful procedure for the analysis and the optimization of the thermal performance of a flat solar plate collector (FSPC) with thermosiphon. The obtained results are as follows:

The increase of the fluid outlet temperature with the exergy efficiency and the decrease of the mass flow rate are not signs of the good functioning of the FPSC because an augmentation of the destroyed exergy is observed. This fact led to carry out an optimization to seek the adequate parameters.

The optimal values were acquired through exergy efficiency optimization: mass flow rate 0.06 kg/s, exergy efficiency 8.28% and energy efficiency 68.74%. The latter are in agreement with the literature ones. A maximum value of the energy efficiency is not always a good sign of the condition of the FPSC. It should be compared with the optimal exergy efficiency. In the Saharan climate, the optimal performance of a solar water heater usually becomes clear in the afternoon. The hypothesis of $T_{fi} \approx T_a$ is not well suited to the exergy study given that this concept is based on the system and on its environment, where any variation in ambient temperature T_a directly influences the results of the calculation of optimal parameters. The results of the exergy analysis enabled us during the design phase to improve the performance of the prototype solar collector. The exergy analysis highlighted the irreversibility or entropy generation, which is often disregarded in energy studies. It plays a key role in understanding, improving and designing energy systems.

Acknowledgment

We wish to extend our great gratitude to Mrs. Wilhelmina Logerais, a mother tongue speaker, for her particular help during the entire process of paper composing and revising.

References

Alim MA, Rahman S, Rahim NA, Alam MK, Fauzan MF, Islam MR, Abdin Z. 2016. Energy and exergy analysis of a flat plate solar collector using different nanofluids. Journal of Cleaner Production **112,** 3915-3926.

Bejan A, Kearney DW, Kreith F. 1981. Second law analysis and synthesis of solar collector systems. Journal of Solar Energy Engineering **103(1),** 23-28.

Bejan A. 1988. Advanced engineering thermodynamics. Wiley Interscience, Nork, New York, USA.

Benli H. 2013. Experimentally derived efficiency and exergy analysis of a new solar air heater having different surface shapes. Renewable Energy **50,** 58-67.

Bennaceur S, Draoui B, Bennamoun L. 2010. Étude expérimentale d'un chauffe-eau solaire au sud-ouest Algérien. Séminaire International sur le Génie Climatique et l' Energétique, SIGCLE' 2010, Constantine, Algeria.

Das S. 2016. Simulation of optimal exergy efficiency of solar flat plate collector. Jordan Journal of Mechanical and Industrial Engineering **10(1),** 51-65.

Dincer Ibrahim, Rosen Marc A. 2013. Exergy energy environment and sustainable development. Elsevier, Second edition.

Eugene D. Coyle, Richard A. Simmons. 2014. Understanding the Global Energy Crisis. Published on behalf of the Global Policy Research Institute by Purdue University Press West Lafayette, Indiana,

Farahat S, Sarhaddi F, Ajam H. 2009. Exergetic optimization of flat plate solar collectors. Renewable Energy **34(4),** 1169-1174.

Feidt M. 1987. Thermodynamique et optimisation énergétique des systèmes et procédés. Tec et Doc Lavoisier, Paris.

Ge Zhong, Huitao Wang, Hua Wang, Songyuan Zhang, Xin Guan. 2014. Exergy analysis of flat plate solar collectors. Entropy **16,** 2549-2567.

Hepbasli Arif. 2008. A key review on exergetic analysis and assessment of renewable energy

resources for a sustainable future". Renewable and Sustainable Energy Reviews **12,** 593-661.

Jeter SM. 1981. Maximum conversion efficiency for the utilization of direct solar radiation. Solar Energy **26(3),** 231-236.

Kalogirou SA, Karellas S, Badescu V, Braimakis K. 2016. Exergy analysis on solar thermal systems: A better understanding of their sustainability. Renewable Energy **85,** 1328-1333.

Kalogirou SA, Karellas S, Braimakis K, Stanciu C, Badescu V. 2016. Exergy analysis of solar thermal collectors and processes. Progress in Energy and Combustion Science **56,** 106-137.

Lallemand A. 2007. Énergie exergie économie thermo-économie. Journées internationales de thermique, hal-00189701, p 30.

Luminosu I, Fara L. 2005. Determination of the optimal operation mode of a flat solar collector by exergetic analysis and numerical simulation, Energy **30,** 731-47.

Petela R. 1964. Energy of heat radiation. Journal of Heat Transfer **86(2),** 187-192.

Said SAM. 1990. Effects of dust accumulation on performances of thermal and photovoltaic flat-plate collectors. Applied Energy **37,** 73-84.

Saidur R, BoroumandJazi G, Mekhlif S, Jameel M. 2012. Exergy analysis of solar energy applications. Renewable and Sustainable Energy Reviews **16,** 350-356.

Semaouia Smail, Hadj-Araba Amar, Boudjelthiaa Elamin Kouadri, Bachab Seddik, Zeraiaa Hassiba. 2015. Dust effect on optical transmittance of photovoltaic module glazing in a desert region". Energy Procedia **74,** 1347-1357.

Shojaeizadeh E, Veysi F. 2016. Development of a correlation for parameter controlling using exergy effciency optimization of an Al2O3/water nanofluid based flat-plate solar collector. Applied Thermal Engineering **98,** 1116-1129.

Singh SK, Rai AK, Sachan V. 2016. Fabrication and performance study of a solar water heater. International Journal of Advanced Research in Engineering and Technology (IJARET) **7(4),** 01-05.

Soteris A. Kalogirou. 2004. Solar thermal collectors and applications. Progress in Energy and Combustion Science **30,** 231-295.

Spanner DC. 1964. Introduction to thermodynamics. Academic Press, London.

Struckmann Fabio. 2008. Analysis of a Flat-plate Solar Collector. Project Report 2008 MVK160 Heat and Mass Transport May 08, Lund, Sweden.

Sukhatme SP, Nayak JK. 2017. Solar energy: Principles of thermal collection and storage. Tata McGraw-Hill Education, 4th edition p. 568.

Suzuki A. 1988. A Fundamental equation for exergy balance on solar collectors. Journal of Solar Energy Engineering **110(2),** 102-106.

Tiwari GN, Shyam A. 2016. Handbook of solar energy theory analysis and applications. Energy Systems in Electrical Engineering, Springer Verlag, Singapore, 1st edition p. 764.

Tohching S, Velautham S, Nordin A. 2007. Exergetic optimization of a flat plate solar collector design. International Energy Journal **8,** 125-130.

Verma SK, Tiwari AK, Chauhan DS. 2017. Experimental evaluation of flat plate solar collector using nanofluids. Energy Conversion and Management **134,** 103-115.

Wencelas KY, Tchuen G. 2017. Optimization of flat-plate solar collectors used in thermosyphon solar water heater. International Journal of Renewable Energy Technology Research **6(2),** 21-23.